HHS Public Access

Author manuscript

Biol Psychiatry. Author manuscript; available in PMC 2016 April 01.

Published in final edited form as:

Biol Psychiatry. 2015 April 1; 77(7): 616–623. doi:10.1016/j.biopsych.2013.07.017.

Anatomical Characteristics of the Cerebral Surface in Bulimia Nervosa

Rachel Marsh, Ph.D.[1,2], **Mihaela Stefan, M.A.**[1], **Ravi Bansal, Ph.D.**[3], **Xuejun Hao**[3], **B. Timothy Walsh, M.D.**[2], and **Bradley S. Peterson, M.D.**[1,3]

[1]The Division of Child and Adolescent Psychiatry in the Department of Psychiatry, the New York State Psychiatric Institute and the College of Physicians & Surgeons, Columbia University, New York, NY

[2]The Eating Disorders Research Unit in the Department of Psychiatry, the New York State Psychiatric Institute and the College of Physicians & Surgeons, Columbia University, New York, NY

[3]The Center for Developmental Neuropsychiatry in the Department of Psychiatry, the New York State Psychiatric Institute and the College of Physicians & Surgeons, Columbia University, New York, NY

Abstract

Objective—To examine morphometric features of the cerebral surface in adolescent and adult females with Bulimia Nervosa (BN).

Methods—Anatomical magnetic resonance images were acquired from 34 adolescent and adult females with BN and 34 healthy, age-matched controls. We compared the groups in the morphological characteristics of their cerebral surfaces while controlling for age and illness duration.

Results—Significant reductions of local volumes on the brain surface were detected in frontal and temporoparietal areas in the BN compared to control participants. Reductions in inferior frontal regions correlated inversely with symptom severity, age, and Stroop interference scores in the BN group.

Conclusion—These findings suggest that local volumes of inferior frontal regions are smaller in individuals with BN compared to healthy individuals. These reductions along the cerebral surface may contribute to functional deficits in self-regulation and to the persistence of these deficits over development in BN.

Address reprints requests to: Rachel Marsh, Ph.D., Columbia University and the New York State Psychiatric Institute, 1051 Riverside Drive, Unit 74, New York, NY 10032. Phone: 212-543-5384; Fax: 212-543-0522; MarshR@childpsych.columbia.edu.

Financial Disclosures

Dr. Walsh receives research support from AstraZeneca and Dr. Peterson receives investigator-initiated funding from Eli Lilly and Pfizer. All other authors report no biomedical financial interests. All authors report no potential conflicts of interest.

Keywords

Bulimia Nervosa; MRI; surface morphology; frontal cortex; eating disorders; frontostriatal

INTRODUCTION

Bulimia Nervosa (BN) typically begins in adolescence, primarily affects females, and is characterized by recurrent episodes of binge-eating that are accompanied by a sense of loss of control and followed by self-induced vomiting or another compensatory behavior to avoid weight gain (1, 2). Mood disturbances and impulsive behaviors are also common in persons with BN, suggesting the presence of pervasive difficulties in behavioral self-regulation (2).

Our previous functional neuroimaging findings from adult women with BN suggest that their failure to engage frontostriatal circuits may contribute to their impaired capacity for self-regulation (3). Our findings from adolescent girls with BN suggest that this circuit-based dysfunction arises early in the course of illness and is therefore unlikely to be an effect of chronic illness (4). We do not know, however, whether anatomical abnormalities in these circuits are associated with deficient frontostriatal functioning in BN or contribute to illness persistence.

Previous anatomical imaging studies of individuals with BN are sparse. Findings from oxel-based morphometric studies of adults with BN vary; some suggest larger grey matter volumes of the orbitofrontal cortex (5, 6) and ventral striatum (6), and others suggest no differences in global or regional grey matter volumes (7) in BN compared to control participants. Finer-grained approaches to assess and spatially localize structural abnormalities, such as measures of cortical thickness and morphological assessment of the cerebral surface, have not been applied to anatomical data collected from individuals with BN. In addition, no prior studies have assessed brain structure in adolescents with BN.

Using methods previously used to assess brain morphology in various psychiatric disorders (8–11), we compared morphological measures of the cerebral surface across adolescent and adult females with BN and age-matched healthy participants. Based on our previous functional findings, we suspected that relative to healthy participants, those with BN would show reductions in local volumes within the surface of the frontal lobe. In exploratory analyses, we assessed group differences in the age correlates of surface measures and whether abnormalities in the frontal regions of individuals with BN were associated with measures of BN symptom severity or with deficits in self-regulatory control, as measured by cognitive interference on a Stroop task (12) performed outside of the MRI scanner.

METHODS

Participants

The sample consisted of 34 adolescents and adults with BN and 34 age-matched control participants who participated in our fMRI studies (3, 4). Those with BN were recruited through flyers posted in the local community and internet advertisements (e.g., craigslist.com and eating disorder-specific websites) and through the Eating Disorders Clinic

at the New York State Psychiatric Institute (NYSPI), where they were receiving treatment. Control participants were recruited through flyers and internet advertisements. All participants were females, group-matched by age and body mass index. Those with a history of neurological illness, past seizures, head trauma with loss of consciousness, mental retardation, pervasive developmental disorder, or current Axis I disorders (other than Major Depression for the patients) were excluded. Controls also had no lifetime Axis I disorders. Formal diagnoses of BN and comorbid neuropsychiatric diagnoses were established using standard adult and child measures (see supplement). All participants received monetary compensation for their participation. The Institutional Review Board of the NYSPI approved this study, and all participants gave informed consent.

MRI Acquisition

MRI scans were acquired on a GE Signa 3 Tesla whole-body scanner with a body transmitter coil and an eight-channel head receiver coil. High-resolution, T1-weighted images were acquired using a fast spoiled gradient-recall 3D pulse sequence: inversion time = 500ms, echo time = 1.3ms, repetition time 4.7 msec, 2 excitations, matrix size = 256 × 256, field of view = 25cm, flip angle = 11, number of slices = 164, slice thickness = 1mm encoded for sagittal slice reconstruction, providing voxel dimensions of 0.976 × 0.976 × 1.0mm.

Image Processing

Morphometric analyses were conducted blind to participant characteristics and hemisphere (images were randomly flipped in the transverse plane prior to preprocessing) on Sun Ultra 10 workstations using ANALYZE 9.0 (Rochester, MN).

Preprocessing Large-scale variations in image intensity were corrected (21) and extra-cerebral tissues were removed by an automated tool (22) before connecting dura was removed manually on each sagittal slice and checked in orthogonal views.

Cortical gray matter segmentation Gray-scale values of “pure” representations of cortical gray and white matter were sampled bilaterally in frontal, temporal, occipital, and parietal regions using an 8 × 8 = 64 pixel array that was sufficiently large enough for statistical stability but small enough to avoid partial volume effects from other tissue types. These four values were averaged for each tissue type, and a threshold value (halfway between the gray and white matter values) was applied to each slice in the imaging volume to provide an initial classification of gray and white matter that was then hand edited in coronal and transverse views. The intraclass correlation coefficient, calculated using a 2-way random-effects model (23) as a measure of reliability of our segmentation procedures, was 0.98.

Choice of template brain We applied a rigorous two-step procedure to select template brain most representative of our control sample (24). We first selected as a preliminary reference the brain of a healthy participant who was representative of the control sample by age, weight, and height. The brains of the other control participants were coregistered to this preliminary template. Point correspondences on cortical surfaces were determined, and we computed the distance from the template surface for each of the corresponding points on the surfaces of the brains of all the other control participants. The brain for which all points

across the surface were closest to the average of least squares distances was selected as the final template. Brains then underwent a second coregistration to this template. We used a single template rather than an averaged brain because it has well defined-tissue interfaces (e.g., CSF/gray matter or gray/white matter). Averaging images for a template would blur these boundaries, thereby increasing registration errors that could contribute to subtle group differences in morphology.

Morphological maps of the cerebral surface Detailed descriptions and validation of our methods used to analyze morphological features of the cerebral surface are provided elsewhere (24–26). Briefly, the random flips were first reversed to provide their correct left-right orientation. Using a similarity transformation based on mutual information of gray scale values, each brain was coregistered to the template brain such that the cerebral surfaces were moved to a close approximation of the template surface. We then applied to each brain a high-dimensional, nonlinear warping algorithm so that its gray scale intensities matched those of the template brain point by point across the entire cerebrum (11, 24–26), providing a point-wise labeling of the correspondences of the cortical surfaces across all brains in the sample. The high-dimensional, nonlinear warp was then reversed, bringing the labels for point correspondences of the cerebral surface back to the close approximation established by the similarity transformation.

Surface Distances/Local Volumes Signed Euclidian distances from corresponding points across the cerebral surfaces for each participant to corresponding points on the template surface were calculated and subjected to statistical modeling at each voxel. These distances were positive for outward deformations (protrusions) and negative for inward deformations (indentations) of the each participant's surface relative to the template. Thus, indentations or protrusions along the surface were interpreted as representing greater or smaller local volumes, respectively, of brain tissue along those surfaces.

Cortical thickness We masked out the cortical mantle from the coregistered brain of each participant. A 3D morphological operator then distance-transformed each brain without the cortex from the same coregistered brain containing the cortex (27), calculating cortical thickness as the smallest distance of each point on the cortical surface from the outermost surface of white matter in the coregistered brain. Because these thicknesses were scaled for whole brain volume (WBV), the values inherently accounted for general scaling effects and inter-individual differences in WBV.

Stroop Interference

Stroop interference, measured outside the scanner with the standard format of the task (28) (see supplement), was used for correlation analyses with measures of surface morphology. Because the adult (3) and adolescent (4) fMRI participants performed different versions of the Simon task, those behavioral or fMRI data could not be used in these correlation analyses. We therefore used Stroop data, as the Stroop and Simon tasks elicit similar patterns of frontostriatal activations during the engagement of self-regulatory control in healthy individuals (30).

Statistical Analyses

We used general linear modeling to compare the participants with and without BN in cortical morphology. Each imaging measure (Euclidian distances or cortical thickness) was subjected to statistical modeling at each voxel of the surface of the template brain with age as a covariate. P-values were corrected for multiple comparisons using a false discovery rate of 0.05, color-coded and plotted for each voxel on the cerebral surface. In exploratory analyses, we assessed the significance of correlations of distances over the entire cerebral surface with BN symptom severity in the BN group while covarying for age and illness duration, and compared groups in their patterns of correlations with age and with Stroop Interference at each voxel across the cerebral surface.

Results

Participants

Analyses include data from 34 BN and 34 healthy participants, including 16 BN and 16 healthy adolescents (≤19 years). All were right-handed. BN participants included 5 inpatients scanned within one month of admission and 8 outpatients; the remaining BN participants were not seeking treatment (n=11) or no longer receiving treatment in our clinic (n=10), but all were symptomatic. Six presented with sub-clinical BN, with less than 8 (2x/week) objective bulimic episodes (OBEs, N=2), vomiting episodes (N=2), or OBEs and vomiting episodes (N=2) over the past 28 days prior to participation. None met criteria for MDD or ADHD. Ten had a prior diagnosis of Anorexia Nervosa. Twelve were taking SSRIs at the time of scan (Table SI). All participants were postpubertal and menstruating regularly.

Group Differences in Morphology of the Cerebral Surface WBV did not differ across the BN and control groups, either unadjusted (BN vs. control: 1291.7±131.8 vs. 1,310±130.7 cm^3, $t_{(66)}$=−0.57, p=0.65) or adjusted for age and BMI (1289.9±25.9 vs. 1,312±25.9 cm^3, $F_{(1,64)}$=0.52, p=0.47). Nevertheless, the BN group had significant reductions in local volumes of bilateral middle frontal (MFG) and precentral gyri (PreCG), right postcentral gyrus (PoCG), and lateral superior (SFG) and inferior frontal gyri (IFG) of the left hemisphere (Fig. 1). Analyses of white matter demonstrated that these reductions on the cerebral surface of the frontal lobe in the BN group derived primarily from reductions of underlying white matter (Fig. 2). Reductions were also detected in temporoparietal areas, including bilateral inferior temporal gyri, right superior parietal gyrus (SPG) and cuneus, as well as bilateral posterior cingulate cortices (PCC), left precuneus, and fusiform gyrus. In addition, enlargements were detected in bilateral middle/inferior occipital and lingual gyri, and right inferior parietal lobule (IPL) in the BN vs. control groups, deriving from enlargements in underlying white matter (Fig. 2).

Group Differences in Cortical Thickness Scattered reductions in cortical thickness in bilateral dorsal and lateral frontal, parietal, and posterotemporal cortices in the BN vs. control groups (Fig. S1) were consistent with the locations of group differences in cortical morphology.

Correlations with Symptom Severity and Impulsivity Within the BN group, we detected significant inverse associations of cerebral surface morphology with log transformed (31)

objective bulimic and vomiting episodes in bilateral IFG, PreCG, and PoCG (Figs. 3& S2). Scatterplots of these associations suggested greater reductions of these areas in those who engaged in the most episodes within 28 days prior to scanning. Inverse associations with participant ratings of their preoccupation with shape and weight in bilateral IFG, right PoCG, and left medial frontal gyrus (MFG, Fig. S3) suggested greater reductions in the most preoccupied BN participants. Impulsivity in the BN group, measured with three items targeting impulsivity on the ADHD rating scale, correlated inversely with surface morphology in left IFG and medial temporal gyrus (MTG, Fig. S4).

Effects of Age and Illness Duration Significant diagnosis-by-age interactions on cortical surface morphology were detected in MFG and IFG of the left hemisphere and in the PoCG of the right hemisphere (Fig. 4). Scatterplots of these interactions indicated that age correlated significantly and inversely with local volume reductions in the BN but not the control group in these brain areas. Diagnosis-by-age interactions were also detected in bilateral IPL such that age correlated inversely with reductions in the control but not the BN group. Separate maps of age effects in each group revealed that age correlated inversely with reductions in right IFG and MFG in controls and in large expanses of bilateral inferior frontotemporal regions in the BN group (Fig. S5). Because age and illness duration were significantly intercorrelated in the BN group ($r=0.89$; $p=0.001$), we controlled for illness duration effects on surface morphology using a subgroup of 21 BN participants in whom age and illness duration were uncorrelated ($r=0.36$; $p=0.10$) and a subgroup of 18 age-matched controls. Diagnosis-by-age interactions remained in left IFG and MFG, and were additionally detected in left PreCG, MTG and superior temporal gyrus (STG), and right IFG, as well as right cingulate (CG) and left SFG (Fig. S6) on the mesial surface; age correlated inversely with reductions in the BN but not the control subgroup in these areas. Age also correlated inversely with reductions in right IPL, and positively with enlargements in right SFG in the BN but not the control subgroup (Fig. S6). Illness duration in the BN subgroup correlated inversely with reductions in right IFG, bilateral MFG, IPL, occipital cortices and CG (Fig. S7).

Interactions of Diagnosis × Stroop Interference The BN and control groups performed similarly on the Stroop task (Table 1). Nevertheless, significant interactions of diagnosis × Stroop interference scores on surface morphology were detected in IFG, MTG, and STG the lateral surface of the left hemisphere; Stroop interference correlated inversely with reductions in the BN but not the control group (Fig. 5).

Medication and Comorbidity Effects After including current SSRI treatment as an independent variable in a separate linear regression, local reductions in bilateral frontal cortices in the BN group remained unchanged from those depicted in figure 1 (Fig. S8), indicating that SSRI treatment did not have an appreciable effect on our findings. Likewise, neither a history of anorexia (Fig. S9) nor current depressive symptoms (Fig. S10) contributed to our findings.

Discussion

Significant reductions in local volumes of the cerebral surface in individuals with BN predominated in frontal and temporoparietal regions, including bilateral MFG and PreCG, SFG and IFG on the lateral surface of the left hemisphere, and bilateral inferior temporal gyri on the ventral surface. On the medial surface, reductions were detected in right fusiform, SPG, and cuneus, left precuneus, and bilateral PCC. Greater reductions in bilateral inferior frontal cortices were detected in the BN participants who engaged in the most objective bulimic and vomiting episodes, and in those who were the most preoccupied with shape and weight. Significant diagnosis-by-age interactions indicated that reductions in MFG and IFG of the left hemisphere and in the PoCG of the right hemisphere became more prominent with advancing age in the BN but not the control participants. Conversely, interactions with age in bilateral IPL indicated age-related volume reductions that were more prominent in the healthy than in the BN participants, consistent with the overall enlargement of the right IPL in the BN vs. control group. Analysis of a BN subgroup revealed that reductions in right, but not left, IFG, bilateral IPL and CG were associated with illness duration rather than age. Significant interactions of diagnosis with Stroop interference scores in IFG, MTG, and STG of the left hemisphere suggested that greater Stroop interference accompanied greater regional reductions, consistent with the interactions with age at these locations.

Our previous fMRI findings from adult (3) and adolescent (4) females indicated deficient activation of frontal areas compared to age-matched control participants during performance of a self-regulatory task. The current findings suggest that morphological abnormalities, specifically reductions in local volumes of inferior frontal lobes, are associated with, and may underlie, these deficits in self-regulation that characterize individuals with BN and likely contribute to their impaired control over feeding and other behaviors. These reductions were detected in bilateral MFG and PreCG, and left IFG, consistent with a previous report of significantly lower T1 relaxation times in BN vs. control participants in inferior frontal gray matter (32). Inverse associations of objective bulimic and vomiting episodes with surface measures were detected in bilateral IFG, PreCG, and PoCG, suggesting that reductions in bilateral frontal cortices may be required for individuals to manifest the greatest loss of control over feeding behaviors and, therefore, the most severe BN symptoms. Inverse correlations of surface measures with participant ratings of their preoccupation with shape and weight were detected in right PreCG, left MFG, and bilateral IFG, indicating the degree of reduction was related to the severity of the shape/weight concern characteristic of BN. The right IFG typically activates during successful response inhibition in healthy individuals (33–35) and is therefore implicated in supporting the capacity for self-regulatory control. Individuals with BN, however, either deactivate (4) or activate IFG less than control participants (3) during a task of self-regulatory control. Although the relationship between structure-function is far from clear, we suspect that both structural and functional deficits in this ventral (inferior frontal) attentional (36) and regulatory system are centrally involved in the pathogenesis of BN.

We also detected volume reductions in left precuneus, right cuneus, and SPG on the medial surface that derived primarily from reductions in underlying white matter, consistent with

recent findings of reduced white matter in women with BN in right temporoparietal areas compared to control participants (5). Those findings were interpreted based on insula-related brain circuitry in eating disorders, given the fiber paths that connect temporal areas with the insula and PFC (37). We did not assess insular morphology, but insula circuit-based abnormalities, including white matter reductions in connected temporal regions, may contribute to altered self-perceptions (38, 39) of body image in BN. Both precuneus (40) and PCC are implicated in self-awareness and mental imagery about the self, constituting part of the default mode network (DMN) of brain areas that activate during engagement in internally-driven thoughts (41). We previously detected DMN deactivations in BN adolescents when performing a regulatory control task (4), a finding we attributed to their allocating attention to internally-driven thoughts about eating or body image that preoccupy individuals with BN. Thus, volume reductions in these areas may contribute, in part, to excessive DMN deactivation during fMRI task performance and the tendency of BN adolescents to attend to internally-driven thoughts. However, task-related deactivation of DMN is analogous to its activation when engaged in internally driven thoughts, so such thoughts would likely produce activity-dependent hypertrophy rather than the reductions in precuneus and PCC we observed in the BN group. In addition, ratings of preoccupation with shape/weight did not correlate with reductions in precuneus or PCC, a finding that would suggest hypoplasia rather than hypertrophy in those who engaged most in internally-driven thoughts about their bodies. Thus, unlike our findings of reductions in inferior frontal cortices, reductions in precuneus and PCC are either unassociated with functional deficits in BN or, if associated, not detected herein.

Regional reductions of left MFG and IFG and right PoCG correlated inversely with age in the BN but not healthy participants (Fig. 4). After controlling for illness duration in the BN group, these inverse age correlations remained in left IFG and MFG, and were additionally detected in right IFG and CG, left PreCG, SFG, MTG, and STG (Fig. S6). These reductions became more prominent with age in the BN but not the control group and may represent an abnormal developmental trajectory in BN, such as accelerated grey matter loss, axonal pruning, or reduced myelination. Illness duration was associated with reductions in bilateral occipital cortices and IPL, and in right, but not left, IFG and CG. Reductions in left IFG, MTG and STG correlated inversely with Stroop interference in the BN but not the control group, suggesting that these reductions may have functional consequences for individuals with BN, contributing to their inability to self-regulate their feeding and other behaviors. Consistent with previous behavioral findings (42–44), Stroop interference did not differ between the BN and control groups. Thus, our interpretation of these brain-behavior associations were not confounded by group differences in performance (45). Right frontal activations during Stroop performance increase over development in healthy individuals (34), consistent with the late maturation of frontal cortex (46) and right hemisphere dominance over attentional control (47). Abnormal maturation of left, but not right, frontal cortex, perhaps due to reduced myelination, could therefore contribute to the inefficiency of these brain regions in the service of self-regulation over development in BN.

We previously speculated that deficient frontostriatal activation in individuals with BN may contribute to their general impulsivity and inability to regulate feeding and other impulsive behaviors (48, 49) such as substance abuse (50) and self harm behaviors (51). Impulsivity

correlated inversely with surface morphology in left IFG and PreCG and bilateral MFG (Fig. S4). Healthy individuals engage both right (33–35) and left (52) IFG during successful response inhibition on fMRI measures of impulsivity in healthy individuals. Our fMRI findings suggest that both adolescents and adults with BN fail to activate right IFG, but adolescents deactivate left IFG during successful response inhibition. Perhaps functional and anatomical abnormalities in left inferior frontal cortices arise early in the course of BN and associated with the greater impulsivity in BN vs. healthy adolescents (53), consistent with the effects of illness duration detected in right IFG. These effects were also detected in right MFG and CG (Fig. S7), suggesting that additional reductions in right frontal regions may be due to chronic illness. Future longitudinal imaging studies of BN adolescents with BN, beginning at illness onset, are required to further disentangle the effects of age and illness duration on the structural and functional maturation of frontal cortices in BN.

MRI cannot inform directly our understanding of the cellular changes (e.g., synaptic pruning, myelination) that contribute to brain development. However, our additional analyses of white matter suggested that the reductions in frontal brain volumes in the BN group derived primarily from reductions in underlying white matter (i.e., the reductions in frontal volumes (Fig. 1) were detected in the same locations those detected on white matter (Fig. 2)). Healthy brain development involves both increases in synaptic pruning and myelination over adolescence and young adulthood (54). Greater synaptic pruning over development in BN compared to healthy individuals would manifest as greater reductions in frontal gray matter with increasing age in BN and more efficient processing. More axonal pruning or less myelination, in contrast, would contribute to reductions in white matter with increasing age in BN and less efficient processing, consistent with of fMRI findings from these BN participants. Future longitudinal diffusion tensor imaging studies could confirm the presence of age-related reductions in white matter, and offer an additional explanation for impaired self-regulation during development in BN, as myelination is thought to enhance the speed of the transmission of information and, hence, age-related improvements in cognition (54).

Although the largest anatomical study and only study of the morphological features of the cerebral surface in individuals with BN to date, this study is limited nevertheless by a modest sample size and cross-sectional design. In addition, our BN sample was heterogeneous in symptom severity, and participants were at differing stages of treatment. Moreover, we did not account for menstrual status, which can affect neural functioning in women (55), but we have no reason to suspect that menstrual status differed systematically across the BN and control groups to confound our findings.

Future longitudinal studies comparing brain development in BN and healthy adolescents, beginning at illness onset, are required to determine whether our cross-sectional findings of age-related reductions in inferior frontal volumes represent neurodevelopmental abnormalities in BN or effects of chronic illness on brain structure. Inclusion of a group of individuals with AN in such a study would allow assessment of how brain maturation differs across eating disorders. Identification of atypical neurodevelopmental trajectories in the structure/function of inferior frontal cortices in BN would then warrant development of early interventions aimed at bolstering their functioning. Finally, future studies should analyze the

surface morphology of striatal structures in BN to determine whether reductions or enlargements in the dorsolateral putamen, for example, could contribute to functional abnormalities in habit learning (56), thereby explaining why the binge-eating behaviors in BN tend to crystalize into maladaptive habits.

Supplementary Material

Refer to Web version on PubMed Central for supplementary material.

Acknowledgments

This work was supported in part by NIMH grants K01-MH077652 and R01MH090062, by a grant from the National Alliance for Research on Schizophrenia and Depression (NARSAD), and by funding from the Sackler Institute for Developmental Psychobiology, Columbia University.

References

1. Walsh BT, Klein DA. Eating disorders. International Review of Psychiatry. 2003; 15:205–216. [PubMed: 15276960]
2. Kaye, W.; Strober, M.; Jimerson, DC. The neurobiology of eating disorders. In: Charney, D.; Nestler, EJ., editors. The neurobiology of mental illness. New York: Oxford Press; 2004. p. 1112-1128.
3. Marsh R, Steinglass JE, Gerber AJ, O'Leary KG, Walsh BT, Peterson BS. Deficient Activity in the Neural Systems that Mediate Self-Regulatory Control in Bulimia Nervosa. Arch Gen Psychiatry. 2009; 66:1–13.
4. Marsh R, Horga G, Wang Z, Wang P, Klahr KW, Berner LA, et al. An FMRI study of self-regulatory control and conflict resolution in adolescents with bulimia nervosa. Am J Psychiatry. 2011; 168:1210–1220. [PubMed: 21676991]
5. Frank GK, Shott ME, Hagman JO, Mittal VA. Alterations in Brain Structures Related to Taste Reward Circuitry in Ill and Recovered Anorexia Nervosa and in Bulimia Nervosa. Am J Psychiatry. 2013
6. Schafer A, Vaitl D, Schienle A. Regional grey matter volume abnormalities in bulimia nervosa and binge-eating disorder. Neuroimage. 2010; 50:639–643. [PubMed: 20035881]
7. Joos A, Kloppel S, Hartmann A, Glauche V, Tuscher O, Perlov E, et al. Voxel-based morphometry in eating disorders: correlation of psychopathology with grey matter volume. Psychiatry Res. 182:146–151. [PubMed: 20400273]
8. Bansal R, Staib LH, Laine AF, Hao X, Xu D, Liu J. Anatomical brain images alone can accurately diagnose chronic neuropsychiatric illnesses. PLoS One. 2012; 7:e50698. [PubMed: 23236384]
9. Peterson BS, Warner V, Bansal R, Zhu H, Hao X, Liu J. Cortical thinning in persons at increased familial risk for major depression. Proc Natl Acad Sci U S A. 2009; 106:6273–6278. [PubMed: 19329490]
10. Sobel LJ, Bansal R, Maia TV, Sanchez J, Mazzone L, Durkin K. Basal ganglia surface morphology and the effects of stimulant medications in youth with attention deficit hyperactivity disorder. Am J Psychiatry. 2010; 167:977–986. [PubMed: 20595414]
11. Peterson BS, Choi HA, Hao X, Amat JA, Zhu H, Whiteman R. Morphologic features of the amygdala and hippocampus in children and adults with Tourette syndrome. Arch Gen Psychiatry. 2007; 64:1281–1291. [PubMed: 17984397]
12. Stroop JR. Studies of interference in serial verbal reactions. J Exp Psychology. 1935; 18:643–662.
13. First, MB.; Spitzer, RL.; Gibbon, M.; Williams, JBW. Structured Clinical Interview for DSM-IV-TR Axis I Disorders, Research Version, Non-Patient Edition (SCID-I/NP). New York: Biometrics Research, New York State Psychiatric Institute; 2002.
14. Kaufman J, Birmaher B, Brent D, Rao U, Flynn C, Moreci P. The Schedule for Affective Disorders and Schizophrenia for School Aged Children: Present and Lifetime Version (K-SADS-PL): Initial

reliability and validity data. J Am Acad Child Adolesc Psychiatry. 1997; 36:980–988. [PubMed: 9204677]

15. Cooper Z, Fairburn CG. The Eating Disorder Examination: a semistructured interview for the assessment of the specific psychopathology of eating disorders. Int J Eat Disord. 1987; 6:1–8.
16. Beck, AT.; Steer, RA.; Brown, GK. Beck Depression Inventory Manual. 2. San Antonio, TX: The Psychological Corporation; 1996.
17. Hamilton MAX. Development of a Rating Scale For Primary Depressive Illness. British Journal of Social & Clinical Psychology. 1967; 6:278–296. [PubMed: 6080235]
18. Poznanski EO, Freeman LN, Mokros HB. Children's Depression Rating Scale Revised. Psychopharmacology Bulletin. 1985; 21:979–989.
19. DuPaul GJ. Parent and teacher ratings of ADHD symptoms: psychometric properties in a community-based sample. Journal of Clinical and Child Psychology. 1991; 20:245–253.
20. Wechsler, D. Wechsler Adult Intelligence Scale-Revised. San Antonio, TX: The Psychological Corporation. Harcourt Brace Jovanovich, Inc; 1981. WAIS-R Manual.
21. Sled JG, Zijdenbos AP, Evans AC. A nonparametric method for automatic correction of intensity nonuniformity in MRI data. IEEE Transactions on Medical Imaging. 1998; 17:87–97. [PubMed: 9617910]
22. Shattuck DW, Leahy RM. BrainSuite: an automated cortical surface identification tool. Med Image Anal. 2002; 6:129–142. [PubMed: 12045000]
23. Shrout PE, Fleiss JL. Intraclass correlations: Uses in assessing rater reliability. Psychological Bulletin. 1979; 86:420–428. [PubMed: 18839484]
24. Rauh VA, Perera FP, Horton MK, Whyatt RM, Bansal R, Hao X. Brain anomalies in children exposed prenatally to a common organophosphate pesticide. Proc Natl Acad Sci U S A. 2012; 109:7871–7876. [PubMed: 22547821]
25. Bansal R, Staib LH, Whiteman R, Wang YM, Peterson BS. ROC-based assessments of 3D cortical surface-matching algorithms. Neuroimage. 2005; 24:150–162. [PubMed: 15588606]
26. Plessen KJ, Bansal R, Zhu H, Whiteman R, Amat J, Quackenbush GA. Hippocampus and amygdala morphology in attention-deficit/hyperactivity disorder. Arch Gen Psychiatry. 2006; 63:795–807. [PubMed: 16818869]
27. Haralick, R.; Shapiro, L. Computer and Robot Vision. Vol. Chapter 5. Adison-Wesley Publishing Company; 1992.
28. Lezak, MD. Neuropsychological assessment. 3. New York: Oxford University Press; 1995.
29. Golden, CJ. Stroop Color and Word Test: A Manual for Clinical and Experimental Uses. Wood Dale, IL: Stoelting; 1978.
30. Peterson BS, Kane MJ, Alexander GM, Lacadie C, Skudlarski P, Leung HC. An event-related functional MRI study comparing interference effects in the Simon and Stroop tasks. Brain Res Cogn Brain Res. 2002; 13:427–440. [PubMed: 11919006]
31. Walsh BT, Wilson GT, Loeb KL, Devlin MJ, Pike KM, Roose SP. Medication and psychotherapy in the treatment of bulimia nervosa. Am J Psychiatry. 1997; 154:523–531. [PubMed: 9090340]
32. Hoffman GW, Ellinwood EH Jr, Rockwell WJ, Herfkens RJ, Nishita JK, Guthrie LF. Brain T1 measured by magnetic resonance imaging in bulimia. Biol Psychiatry. 1990; 27:116–119. [PubMed: 2297548]
33. Rubia K, Smith AB, Brammer MJ, Taylor E. Right inferior prefrontal cortex mediates response inhibition while mesial prefrontal cortex is responsible for error detection. Neuroimage. 2003; 20:351–358. [PubMed: 14527595]
34. Marsh R, Zhu H, Schultz RT, Quackenbush G, Royal J, Skudlarski P. A developmental fMRI study of self-regulatory control. Hum Brain Mapp. 2006; 27:848–863. [PubMed: 16421886]
35. Chambers CD, Garavan H, Bellgrove MA. Insights into the neural basis of response inhibition from cognitive and clinical neuroscience. Neurosci Biobehav Rev. 2009; 33:631–646. [PubMed: 18835296]
36. Corbetta M, Shulman GL. Control of goal-directed and stimulus-driven attention in the brain. Nature Reviews Neuroscience. 2002; 3:201–215.

37. Kucyi A, Moayedi M, Weissman-Fogel I, Hodaie M, Davis KD. Hemispheric asymmetry in white matter connectivity of the temporoparietal junction with the insula and prefrontal cortex. PLoS One. 2012; 7:e35589. [PubMed: 22536413]
38. Critchley HD, Wiens S, Rotshtein P, Ohman A, Dolan RJ. Neural systems supporting interoceptive awareness. Nat Neurosci. 2004; 7:189–195. [PubMed: 14730305]
39. Craig AD. How do you feel--now? The anterior insula and human awareness. Nat Rev Neurosci. 2009; 10:59–70. [PubMed: 19096369]
40. Cavanna AE, Trimble MR. The precuneus: a review of its functional anatomy and behavioural correlates. Brain. 2006; 129:564–583. [PubMed: 16399806]
41. Greicius MD, Krasnow B, Reiss AL, Menon V. Functional connectivity in the resting brain: a network analysis of the default mode hypothesis. Proc Natl Acad Sci U S A. 2003; 100:253–258. [PubMed: 12506194]
42. Alvarez-Moya EM, Jimenez-Murcia S, Moragas L, Gomez-Pena M, Aymami MN, Ochoa C. Executive functioning among female pathological gambling and bulimia nervosa patients: preliminary findings. J Int Neuropsychol Soc. 2009; 15:302–306. [PubMed: 19203440]
43. Brand M, Franke-Sievert C, Jacoby GE, Markowitsch HJ, Tuschen-Caffier B. Neuropsychological correlates of decision making in patients with bulimia nervosa. Neuropsychology. 2007; 21:742–750. [PubMed: 17983288]
44. Van den Eynde F, Guillaume S, Broadbent H, Stahl D, Campbell IC, Schmidt U. Neurocognition in bulimic eating disorders: a systematic review. Acta Psychiatr Scand. 2011; 124:120–140. [PubMed: 21477100]
45. Wilkinson D, Halligan P. The relevance of behavioural measures for functional-imaging studies of cognition. Nat Rev Neurosci. 2004; 5:67–73. [PubMed: 14708005]
46. Gogtay N, Giedd JN, Lusk L, Hayashi KM, Greenstein D, Vaituzis AC. Dynamic mapping of human cortical development during childhood through early adulthood. Proc Natl Acad Sci U S A. 2004; 101:8174–8179. [PubMed: 15148381]
47. Garavan H, Ross TJ, Stein EA. Right hemispheric dominance of inhibitory control: an event-related functional MRI study. Proc Natl Acad Sci U S A. 1999; 96:8301–8306. [PubMed: 10393989]
48. Kaye WH, Frank GK, Meltzer CC, Price JC, McConaha CW, Crossan PJ. Altered serotonin 2A receptor activity in women who have recovered from bulimia nervosa. Am J Psychiatry. 2001; 158:1152–1155. [PubMed: 11431241]
49. Tiihonen J, Keski-Rahkonen A, Lopponen M, Muhonen M, Kajander J, Allonen T. Brain serotonin 1A receptor binding in bulimia nervosa. Biol Psychiatry. 2004; 55:871–873. [PubMed: 15050870]
50. Holderness CC, Brooks-Gunn J, Warren MP. Co-morbidity of eating disorders and substance abuse review of the literature. Int J Eat Disord. 1994; 16:1–34. [PubMed: 7920577]
51. Paul T, Schroeter K, Dahme B, Nutzinger DO. Self-injurious behavior in women with eating disorders. Am J Psychiatry. 2002; 159:408–411. [PubMed: 11870004]
52. Swick D, Ashley V, Turken AU. Left inferior frontal gyrus is critical for response inhibition. BMC Neurosci. 2008; 9:102. [PubMed: 18939997]
53. Kaltiala-Heino R, Rissanen A, Rimpela M, Rantanen P. Bulimia and impulsive behaviour in middle adolescence. Psychotherapy & Psychosomatics. 2003; 72:26–33. [PubMed: 12466635]
54. Marsh R, Gerber AJ, Peterson BS. Neuroimaging studies of normal brain development and their relevance for understanding childhood neuropsychiatric disorders. J Am Acad Child Adolesc Psychiatry. 2008; 47:1233–1251. [PubMed: 18833009]
55. Dreher JC, Schmidt PJ, Kohn P, Furman D, Rubinow D, Berman KF. Menstrual cycle phase modulates reward-related neural function in women. Proc Natl Acad Sci U S A. 2007; 104:2465–2470. [PubMed: 17267613]
56. Packard MG, Knowlton BJ. Learning and memory functions of the Basal Ganglia. Annu Rev Neurosci. 2002; 25:563–593. [PubMed: 12052921]

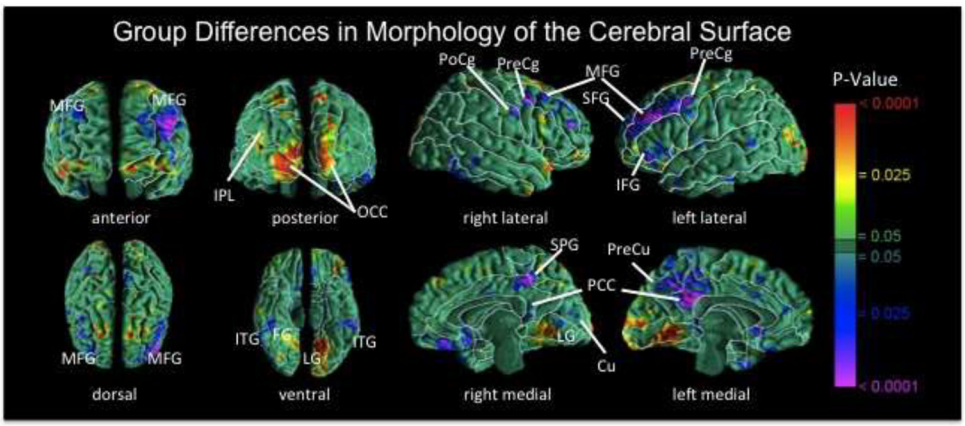

Figure 1. Maps of group differences in morphological measures of the cerebral surface

The signed euclidean distances between points on the surfaces of the cortex for each participant and corresponding points on a template brain were compared statistically between the BN and control groups using linear regression at each voxel on the surface while covarying for age. Warm colors indicate significantly larger distances (local enlargements, outward deformations) in the BN vs. control group; cool colors (blue and purple) indicate reduced distances (local indentations, inward deformations) in the BN vs. control group. The color bar indicates P values corrected for multiple comparisons using a false discovery rate $P < 0.05$. BN group brains were significantly reduced bilaterally in medial frontal and precentral gyri, in superior and inferior frontal gyri of the left hemisphere, the postcentral gyrus of right hemisphere, and bilateral temporoparietal areas (P's = 0.01 to 0.0001). MFG, medial frontal gyrus; PoCg, postcentral gyrus; PreCg, precentral gyrus; IFG, inferior frontal gyrus; SFG, superior frontal gyrus; IPL, inferior parietal lobule; OCC, occipital cortex; ITG, inferior temporal gyrus; FG, fusiform gyrus; SPG, superior parietal gyrus; PCC, posterior cingulate cortex; Cu, cuneus; PreCu, precuneus; LG, lingual gyrus.

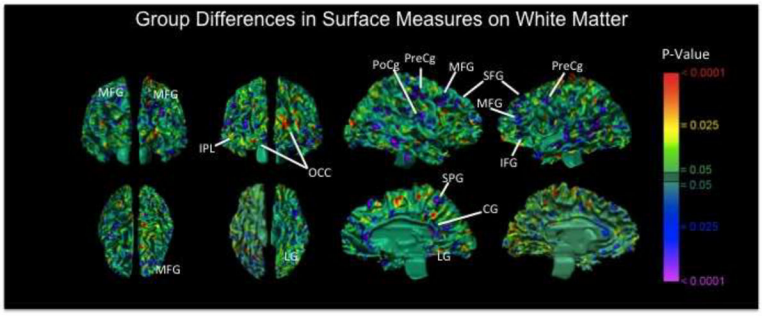

Figure 2. Group differences in surface measures of white matter

Shown here are color-coded maps comparing surface distances of white matter at each corresponding voxel of each participant's brain from the corresponding voxel of the white matter surface in the template brain. The pattern of differences across groups is similar to the pattern of statistical significance of those differences depicted in the maps of P values comparing surface measures on the cerebral surface across groups (Fig. 1), particularly in frontal regions on the lateral surface. These analyses suggest that the observed regional reductions of the cerebral surface in the BN group derived primarily from reductions in underlying white matter.

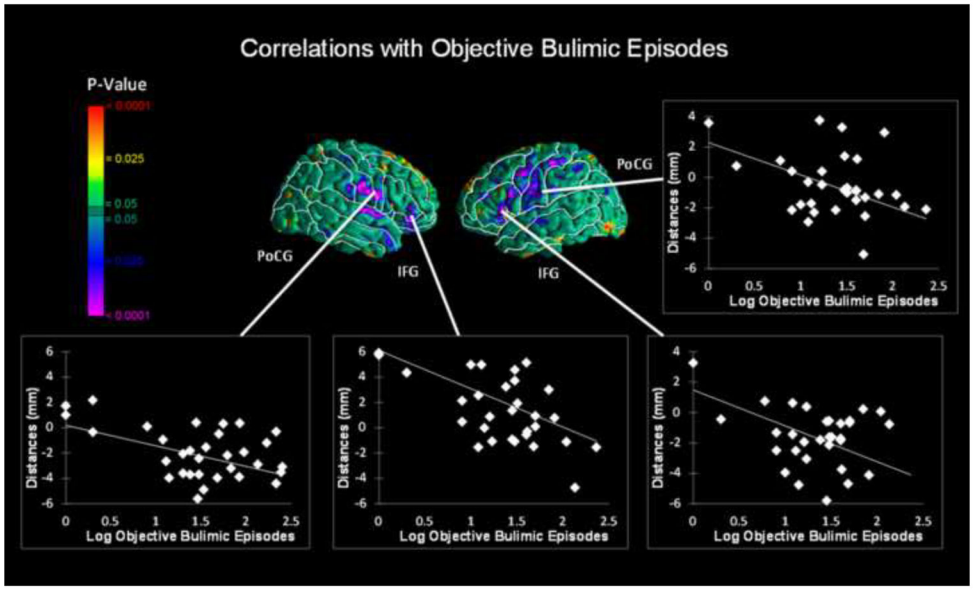

Figure 3. Correlations of cerebral surface morphology with objective bulimic episodes in the BN group

Warm colors (red and yellow) indicate positive correlations and cool colors (blue and purple) indicate inverse correlations between surface measures and objective bulimic episodes within the past 28 days prior to MRI scan. Logarithmic transformations were used to reduce excessive skewness in this frequency variable. Surface distances (in mm from the corresponding point of the template brain), adjusted for age and duration of illness, are plotted on the y axis and log transformed objective bulimic episodes are plotted on the x axis. The scatterplots show greater reductions (larger indentations) in bilateral inferior frontal, pre- and postcentral gyri with more severe symptoms. PreCg, precentral gyrus; PreCg, postcentral gyrus; IFG, inferior frontal gyrus.

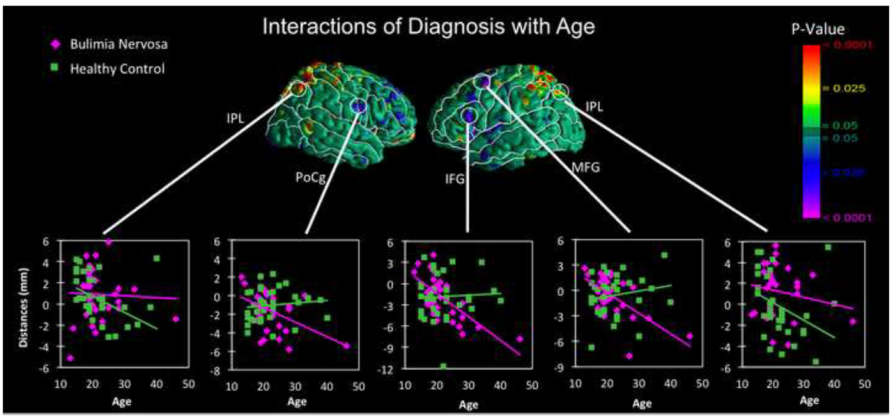

Figure 4. Correlations of surface morphology with age in the BN vs. control groups

Reductions in lateral inferior and medial frontal gyri of the left hemisphere and postcentral gyrus of the right hemisphere correlated inversely with age in the BN but not the healthy participants, producing significant diagnosis-by-age interactions (P's = 0.01 to 0.001). Reductions in inferior parietal lobule, bilaterally, correlated inversely with age in the healthy but not the BN participants, producing significant diagnosis-by-age interactions. Surface distances (in mm from the corresponding point on the surface of the template brain) are plotted on the Y axis. IPL, inferior parietal lobule; MFG, medial frontal gyrus; PoCg, postcentral gyrus; IFG, inferior frontal gyrus.

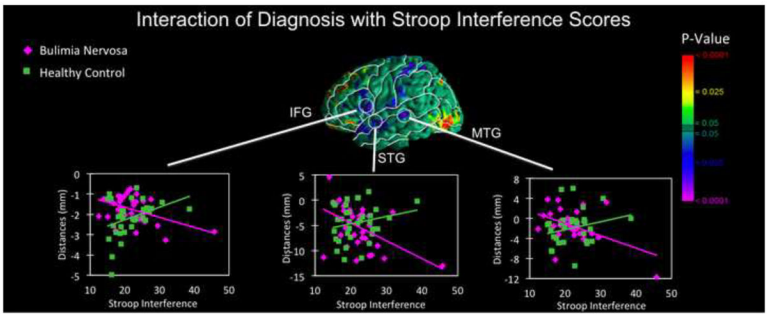

Figure 5. Correlations of surface morphology with Stroop interference scores in the BN vs. control groups

Surface distances (in mm from the corresponding point on the surface of the template brain), adjusted for age, are plotted on the y axis. Reductions in the left inferior frontal gyrus correlated inversely with Stroop interference scores in the participants with BN ($r = -0.7$), producing significant diagnosis × stroop interactions. Scatterplots suggest that greater interference was associated with greater reductions of these regions in the BN group.